Experimental Identification of Undesired Propagation Paths for ETC

Takeo IWATA
Expressway Research Institute, Japan Highway Public Corporation, Tokyo, Japan

Yoshitaka WAKINAKA
Research and Development Institute, Takenaka Corporation, Chiba, Japan

Jun-ichi TAKADA
Department of International Development Engineering, Tokyo Institute of Technology, Tokyo, Japan

Abstract

Electronic toll collection (ETC) service in Japan has been introduced from spring to autumn of 2001. However, it has been found that radio wave signal overreaches outside a specified area, due to multiple reflections of waves between the surface of the road and the canopy, which brought out communication error.

A possible solution to this problem is to install the electromagnetic wave absorber at reflection points of waves. This paper reports our trials of the identification of undesired electromagnetic wave propagation paths using time domain measurement and array signal processing, and shows that we got the measurement results that are in good agreement with calculation results obtained by using ray-tracing in real 2 tollgates.

1. Introduction

Electronic toll collection (ETC) service in Japan has been introduced from spring to autumn of 2001. This service is designed to reduce the traffic congestion at tollgates and to improve the convenience and to reduce the maintenance costs by making toll payments “cashless.” However, it has been found that radio wave signal overreaches outside a specified area, due to multiple reflections of waves between the surface of the road and the canopy, which brought out communication error. A possible solution to this problem is to install the electromagnetic wave absorber at reflection points of waves. Efficiently searching for reflection points of electromagnetic waves, we try to identify propagation paths for undesired electromagnetic wave using time domain measurement and array signal processing. We compare the results of measurement with the results of ray-tracing prediction in 2 tollgates. This report shows the result of our trials.

2. Time domain measurement

Block diagram of time domain measurement is shown in Fig 1. Parameters for the experiments are shown in Table 1. We calibrated the system by setting transmitting and receiving antenna oppositely at 4m distance as shown in Fig.2. We measured the time domain response using network analyzer. Figure 3 shows synthetic array of cube lattice (total 27 points) to measure the space domain response. Interval of lattice points is 2cm, which

corresponds to about 0.45 wavelength at maximum measurement frequency of 6GHz. We set horizontal polarization half-wave dipole tuned for 5.85GHz at lattice points, and moved it to each array point in order, so that we got time domain responses of synthetic array.

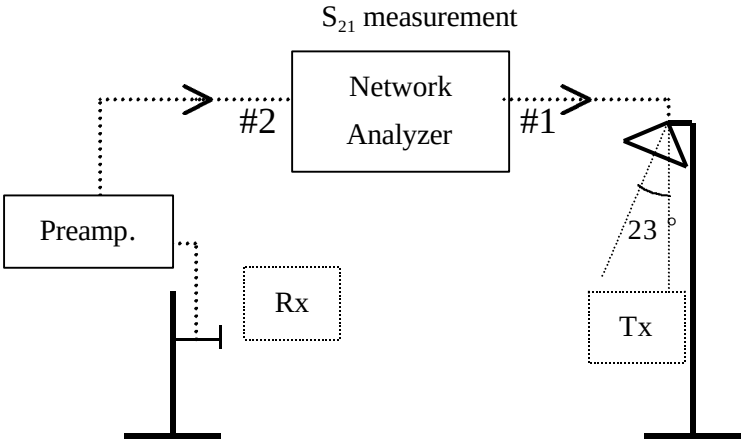

Fig.1 Measurement Block Diagram

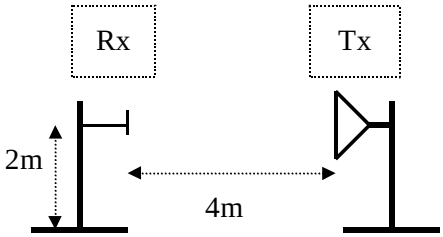

Fig.2 Position of Calibration

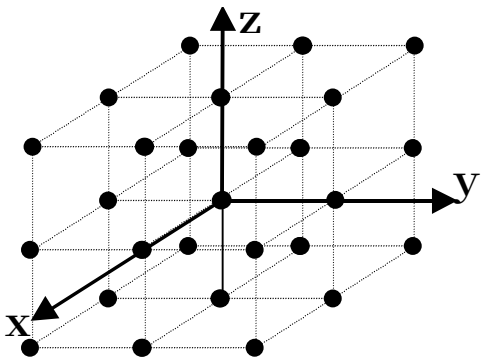

Fig.3 Synthetic array of cube lattice (●：Measurement points)

Table 1 Parameters for the Experiments

Measurement Bandwidth	1GHz － 6GHz
Number of snapshots	16
Average SNR	25dB
Transmitter Antenna (Tollgate Station)	Ridged Horn(245mm×155mm) 5m high, 23 deg tilted from downwards
Receiver Antenna (Mobile Station)	Half-wave dipole for 5.85GHz 1 or 2 m high, horizontally aligned
Time Gate Width	0.8ns
Pre-amplifier Gain	30dB

2. DOA estimation

We selected each specific peak corresponding to the reflected wave in the time domain response at the center point of the array. Its time delay is t. Next, time domain responses at 27 points are gated at the same time delay, so we get transfer functions x_i $(i=1,\ldots,27)$, which compose a data vector $\mathbf{X}$ as

$$\mathbf{X}=[x_1,x_2,\cdots\cdots,x_{27}]^T, \qquad (1)$$

where, T denotes the transpose.

Correlation matrix $\mathbf{R}_{xx}$ is defined as follow.

$$\mathbf{R}_{xx}=E[\mathbf{X}\mathbf{X}^H], \qquad (2)$$

where, $E[*]$ denotes ensemble average, H denotes the Hermitian transpose.

Since the network analyzer automatically average the responses, we used the averaged transfer function instead of ensemble average[1], i.e., $\mathbf{R}_{xx}$ is redefined as Eq. (3).

$$\mathbf{R}_{xx}=E[\mathbf{X}]E[\mathbf{X}^H]. \qquad (3)$$

The array mode vector is defined as follow.

$$\mathbf{a}(q,f)=[\mathbf{r}_1\cdot\mathbf{k},\mathbf{r}_2\cdot\mathbf{k},\cdots,\mathbf{r}_{27}\cdot\mathbf{k}], \qquad (4)$$

where, $\mathbf{r}_i$ $(i=1,2,\cdots,27)$ are position vectors of array elements,

$$\mathbf{k}(q,f)=k_0(\sin q\cos f\hat{\mathbf{x}}+\sin q\sin f\hat{\mathbf{y}}+\cos q\hat{\mathbf{z}})$$

and $k_0=2p/l$,

q and f are elevation and azimuth angles in spherical coordinates, l is wave length, and $\hat{\mathbf{x}},\hat{\mathbf{y}},\hat{\mathbf{z}}$ are unit vectors of x,y,z axis in cartesian coordinates.

Then, the angular spectrum for Beam Forming P_{BF} is defined as [2]

$$P_{BF}(q,f)=\frac{\mathbf{a}^H(q,f)\mathbf{R}_{xx}\mathbf{a}(q,f)}{\mathbf{a}^H(q,f)\mathbf{a}(q,f)}. \qquad (5)$$

We searched peaks of P_{BF} in the ranges of $-90°\sim90°$ for q, and $-180°\sim180°$ for f.

4. Measurement Results

Experimental measurements were done at the real tollgates of the highways in Japan. We compared the results of measurements with the results of ray-tracing prediction in 2 tollgates. Our ray-tracing tool is based on the image method and polygons are used to construct 3-D models[3].

4.1. Result of measurement at tollgate A

In Fig.4, transmitting point (Tx) is located at the center of the lane, with 5m high, and the receiving point (Rx) is located at the center of the lane, with 1m high. Horizontal distance between the transmitting point and the receiving point is 8.5m.

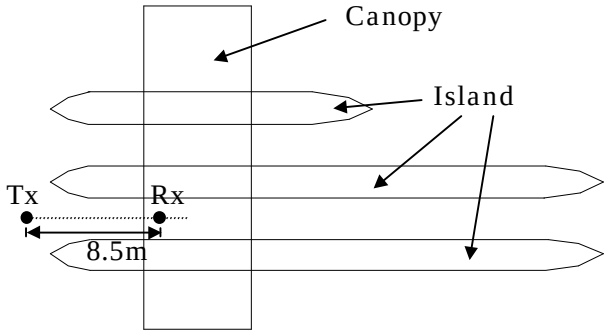

Fig.4 Measurement setup at tollgate A

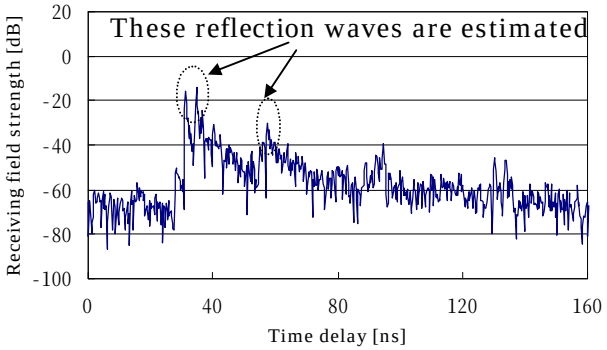

Fig.5 Time domain response at tollgate A

Figure 5 shows the time domain response at the center element of the array. In Fig.5, we estimated 3 peaks corresponding to t =31.3ns, 34.8ns, 57.7ns.

As an example, Fig.6 shows the beaming forming spectrum at t =57.7ns.

Table 2 shows comparison of the ray-tracing and measurement results. The ray numbers in Table 2 correspond to those shown in Fig.7

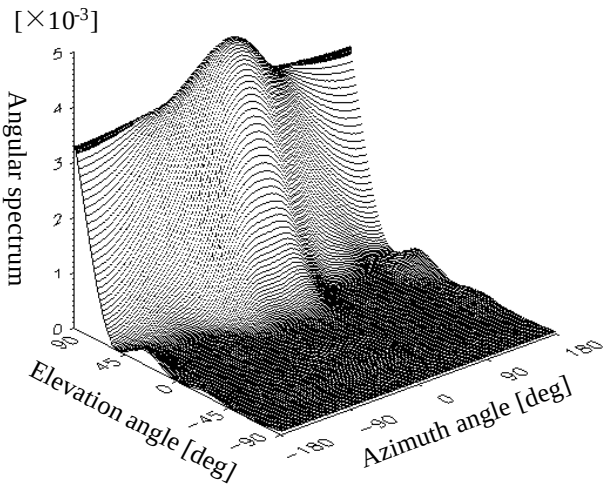

Fig.6 Beam forming spectrum for the DOA estimation at tollgate A, t =57.7ns.

Table 2 Comparison of ray-tracing and measurement results at tollgate A

Ray-tracing prediction						Measurement		
Ray No.	DOA El [deg]	DOA Az [deg]	Delay [ns]	Reflect (1st)	Reflect (2nd)	DOA El [deg]	DOA Az [deg]	Delay [ns]
1	25.2	0.0	31.3	(Direct)		41	−3	31.3
2	−35.2	0.0	34.7	Road		29	−4	34.8
3	67.5	0.0	58.8	Road	Canopy	73	−1	57.7

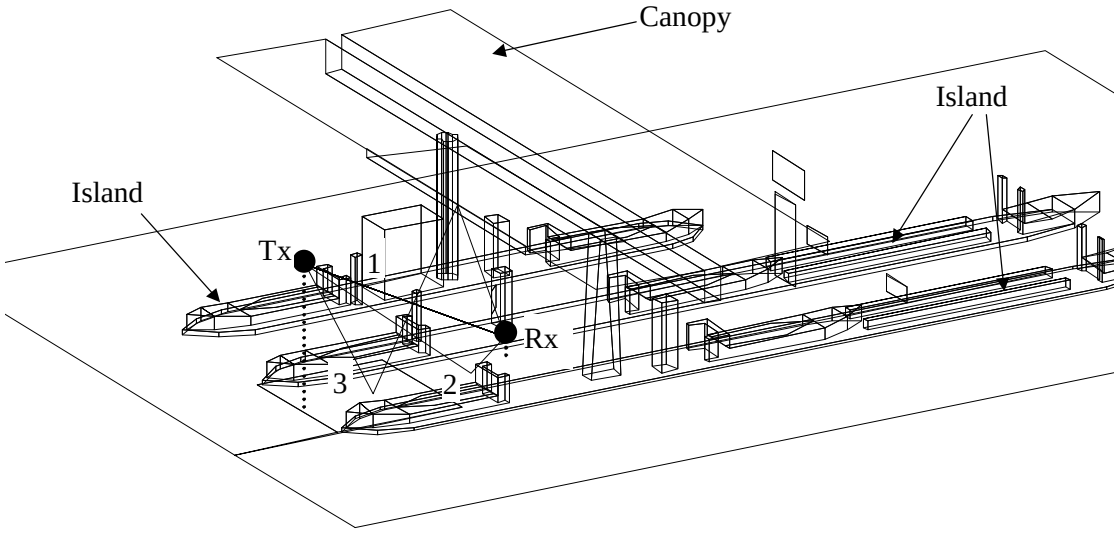

Fig.7 Propagation paths predicted by using ray-tracing at tollgate A.

In Table 2, we found that the DOA differences of the ray-tracing and measurement results are no more than 16 degrees, that is sufficiently small value for the identification.

4.2. Result of measurement at tollgate B

In Fig.8, transmitting point (Tx) is located at the center of the lane, with 5m high, and receiving point (Rx) is located 1.02m offset from the center of the lane, with 2m high. Horizontal distance between transmitting point and receiving point is 9.7m.

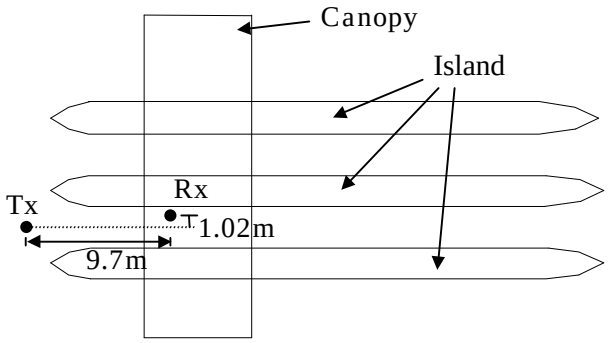

Fig.8 Measurement setup at tollgate B

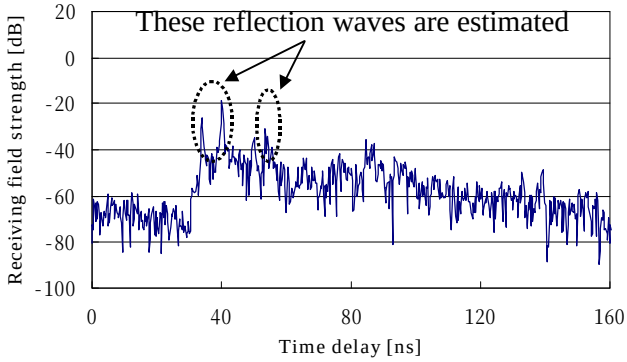

Fig.9 Time domain response at tollgate B.

Table 3 Comparison of ray-tracing and measurement results at tollgate B.

Ray-tracing prediction						Measurement		
Ray No.	DOA El [deg]	DOA Az [deg]	Delay [ns]	Reflect (1st)	Reflect (2nd)	DOA El [deg]	DOA Az [deg]	Delay [ns]
1	17.1	−6.0	34.0	(Direct)		33	−11	34.1
2	−35.7	−6.0	40.0	Road		−24	−12	40.1
3	52.7	−6.0	53.6	Road	Canopy	59	−9	53.7

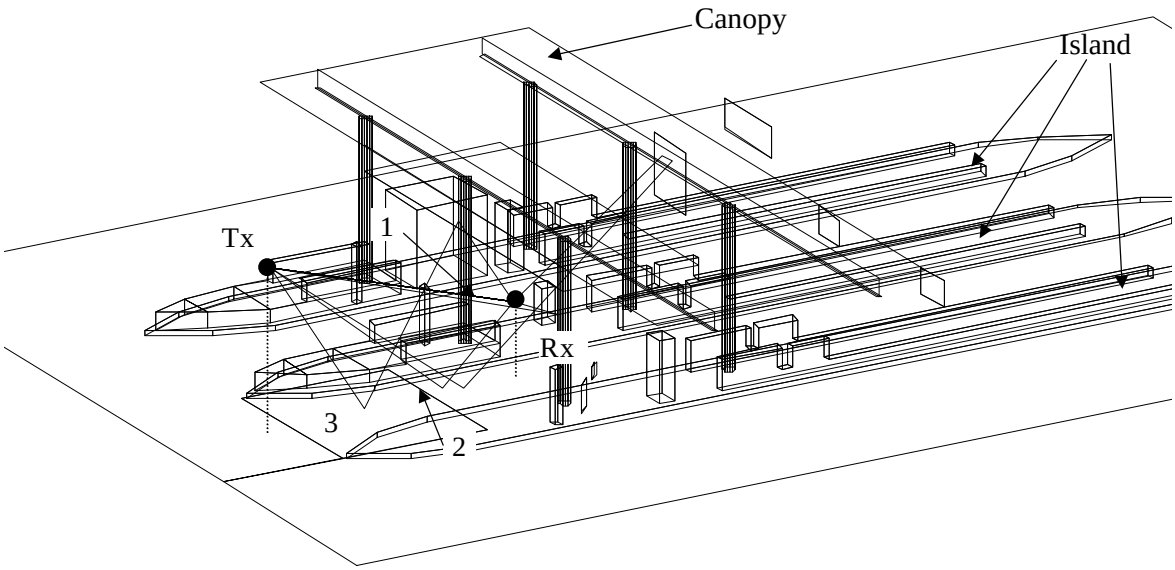

Fig.10 Propagation paths predicted by using the ray tracing at tollgate **B**.

Figure 9 shows the time domain response at the center element of the array. Similar to Fig.5, we estimated 3 peaks corresponding to t =34.1ns, 40.1ns, 53.7ns in Fig.9. As an example, Fig.11 shows the beam forming spectrum at t =53.7ns.

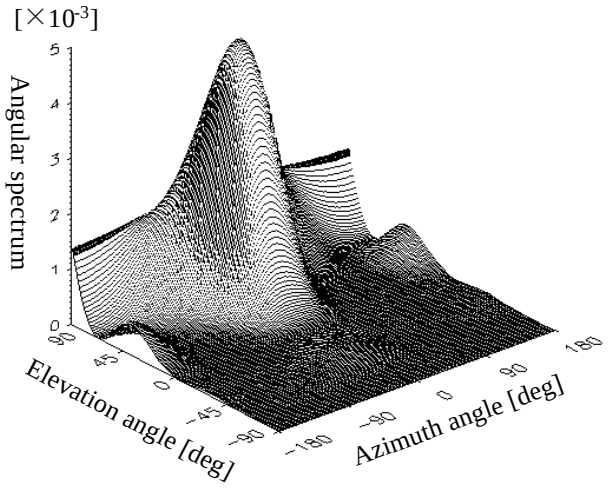

Fig.11 Beam forming spectrum for the DOA estimation at tollgate B, t =53.7ns.

Table 3 shows comparison of ray-tracing and measurement results. The ray numbers in Table 3 correspond to those shown in Fig.7. In Table 3, Similar to section 4.1, we found that the DOA differences of ray-tracing and measurement results are no more than 16 degrees, that is sufficiently small value for the identification.

5. Conclusion

To specify the reflection points of undesired electromagnetic waves for ETC, we tried to identify the propagation paths for the reflection wave using the time delay by time domain measurement and the DOA estimation by array signal processing. In real 2 tollgates, we got the measurement results that are in good agreement with calculation results obtained by using ray-tracing.

Since the rays are identified, the electromagnetic wave absorbers are installed on the canopy and the road at the tollgate to suppress the undesired wave.[4] Figure 12 compares the distribution of electric power before and after the installation of the absorbers at the center of the lane.

6. Acknowledgments

We thank members of Japan Highway Public Corporation Tokyo Third Operation Bureau for their cooperation on the measurements at the tollgates.

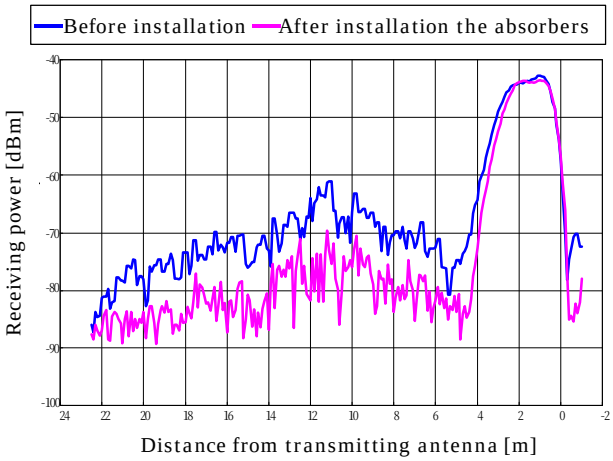

Fig.12 Distribution of electric power before and after installation at the center of the lane

7. References

1) Kohzou OHSHIMA, Yasuhiko TANABE, Yasutaka OGAWA, "A study on Correlation Matrix Calculation for the MUSIC Algorithm", Trans. Of IEICE B, pp.146-149, Vol.J84-B, No.1, Jan., 2001 (in Japanese).

2) Nobuyoshi, Kikuma, "ADAPTIVE SIGNAL PROCESSING with Array Antenna", pp.178-180, Science and Technology pub, 1998 (in Japanese).

3) J. W. McKnown and R. L. Hamilton, "Ray-tracing as a design tool for radio networks," IEEE Networks Mag., pp.21-26, Nov. 1991.

4) Ken-ichi HARAKAWA, Takeo IWATA, Hideo TAKAHASHI, Takeshi KUNISHIMA, "A study of Electromagnetic Environmental Coordination At ETC gates by Wave Absorbers", 8th World Cong. on ITS, Sep. 2001 (to be presented)